ARTICLES

Properties of Silicon Nanoparticles: A Molecular Dynamics Study

Michael R. Zachariah* and Michael J. Carrier

National Institute of Standards and Technology, Gaithersburg, Maryland 20899

Estela Blaisten-Barojas

Institute for Computational Sciences and Informatics, George Mason University, Fairfax, Virginia 22030

Received: December 20, 1995; In Final Form: March 12, 1996[⊗]

Constant energy molecular dynamics simulations of silicon cluster growth have been conducted for clusters up to 480 atoms using the Stillinger−Weber empirical interatomic potential. It is found that the interior atoms of the 480-atom clusters, at the temperatures used, show bulklike characteristics. The cluster binding energy has been fit to an expression that separates the surface and bulk contributions to the energy over wide temperatures and size ranges. The average surface energy of an atom was found to be independent of cluster size and of a magnitude relative to the bulk, such that all cluster sizes were stable under the conditions studied here ($600 < T < 2000$ K). The photon density of states is similar to bulk silicon and does not show a strong cluster size dependence. Atomic self-diffusion coefficients have been calculated and compare quite well with experimental data on self-diffusion coefficient measurements of silicon surfaces.

Introduction

Nanometer processing is receiving considerable interest from a variety of communities, including those from microelectronics and advanced materials. One of the challenges in these areas is the processing of very fine particles. This would include their controlled growth, chemical reactivity, and transport properties. Considerable attention has been paid to the growth of particles in the range of 100 nm and up; however, process modelers have implicitly assumed that small particle growth is unimportant. These issues have however reemerged due to the interest in nanometer particle processing.[1] Understanding the underlying physics and chemistry is necessary for the construction and application of robust phenomenological models for describing particle formation.[2] This is important from the perspective of both the microelectronics community which hopes to minimize particle growth in the vapor during chemical vapor deposition and the ceramics community which hopes to develop the ability to grow from the vapor, spherical, unagglomerated nanometer scale particles.[3−5] Questions regarding the nature of cluster growth kinetics and morphology are of concern. While a large body of literature exists on calculations of the properties of bulk silicon, a much smaller amount of work has been directed toward silicon clusters containing hundreds of atoms. In the cluster studies, the majority of the research involves silicon clusters with 20 atoms and fewer[6−20] with the remainder extending the range to about 50 atoms,[21−29] with no attempt to extend the sizes to what could be called nanoscale materials. In this work we extend the size range of calculation to much larger ($N = 480$) clusters and treat a wide range of temperatures ($600 < T < 2000$ K).

Computational Method

The approach used in this work is to apply an atomistic simulation using classical molecular dynamics (MD) methods.[21,22] The molecular dynamics calculations were conducted by solving the equations of motion with the velocity form of the Verlet algorithm,[30] with a time step of 5.7×10^{-4} ps to ensure energy conservation. Computations were conducted using the silicon potential proposed by Stillinger and Weber (SW).[31] This empirical potential contains two- and three-body interactions which take into consideration the directional characteristic of the covalent bonding and are given in eqs 1a−1c.

$$v = \sum_{\substack{i,j \\ i<j}} v_2(i,j) + \sum_{\substack{i,j,k \\ i<j<k}} v_3(i,j,k) \tag{1a}$$

two-body term

$$v_2(r) = A(Br^{-p} - r^{-q}) \exp[(r-a)^{-1}], \quad r < a$$
$$= 0, \; r \geq a \tag{1b}$$

three-body term

$$v_3(\mathbf{r}_i,\mathbf{r}_j,\mathbf{r}_k) = h(r_{ij},r_{ik},\theta_{jik}) + h(r_{ji},r_{jk},\theta_{ijk}) + h(r_{ki},r_{kj},\theta_{ikj})$$

$$h(r_{ij},r_{ik},\theta_{jik}) = \lambda \exp[\gamma(\mathbf{r}_{ij} - a)^{-1} + \gamma(\mathbf{r}_{ik} - a)^{-1}] \cos(\theta_{jik} + {}^1/_3)^2 \tag{1c}$$

where r is the distance between a pair of atoms, a is the cutoff distance of the two-body potential, and θ_{ijk} is the bond angle between a triplet of atoms. The parameters (A, B, p, q, λ, γ) are constants formulated by Stillinger and Weber and are specific to liquid silicon.[31] While this potential does have some limitations, it is among the best in the literature for representing high-temperature properties of silicon.[12] The diamond crystal

* To whom correspondence should be addressed. E-mail: mrz@tiber.nist.gov.

[⊗] Abstract published in *Advance ACS Abstracts,* July 15, 1996.

S0022-3654(95)03773-7

structure of silicon may be thought of as a network of bonds due to "many-body" effects that a pairwise interatomic potential cannot realistically reproduce. While other potentials are available to simulate silicon, most have been developed for specific purposes, such as accurately reproducing the geometries of very small clusters or specific surface faces, and are generally not as thoroughly tested as SW. The SW potential was chosen because it accurately predicts the elastic constants and cohesive energy of the diamond structure of silicon. It also does well in predicting the bulk melting characteristics and structure of liquid silicon and is one of the most extensively applied silicon potentials for large-scale systems. The SW potential has also been shown to yield a good description of phonon frequencies, as well as surface epitaxial growth at high and intermediate temperatures. While it is well-known that the SW potential does not give accurate structures for very small (<15 atoms) Si clusters at 0 K,[14,15] it does get the correct structure for bulk liquid Si.[12] Because most synthesis processes leading to cluster formation occur at high temperatures, it was felt that liquidlike characteristics should play a dominant role in any description of cluster growth. Our objective is to look at particles created in high-temperature processes which are either liquid or at nearly melted conditions. Since the SW potential has been shown to be useful in studies of bulk liquid, and because our interest lies more toward higher temperatures and increasingly larger cluster sizes, we believe there is justification in the claim that SW results for clusters improve as they get larger and hotter. We are using unterminated clusters in this work for two reasons. First, we are currently investigating the formation of silicon nanoparticles via reaction of Na with $SiCl_4$ where no hydrogen is involved. Second, this is a prelude to an investigation on the coalescence behavior of silicon clusters where it is hoped that extracting phenomenological relationships about particle sintering will be simpler in a single-component system. Furthermore, the work can be related more easily to other metal systems.

The simulations are conducted in two stages:

1. Cluster Preparation/Equilibration. Liquid cluster configurations of 30, 60, 120, 240, and 480 atoms were generated from a related study of cluster−cluster collisions. These were used as a starting point for the creation of the clusters used in this work. The first step in the equilibration process was to remove any angular momentum from the cluster. On average, however, the angular momentum only contributed approximately 5 K to the temperature of the cluster. The cluster was then set to the desired temperature using constant temperature molecular dynamics for a period of 50 ps. At the end of this time segment the simulation was switched to constant energy for 20 ps, and the temperature was recorded over that interval. If the average temperature of the cluster did not change more than 10 K over this period, the equilibration was considered a success; otherwise, the process was repeated.

2. Cluster Property Simulation. Following equilibration, cluster properties were averaged using constant energy molecular dynamics over a period of 25 ps.

Cluster Structure: Surface vs Bulk. Before we embark on an analysis of the internal energy and properties of these clusters, we define more clearly the exact structural nature of the clusters prepared here. The shapes of the clusters used in this work are all spherical as this is the equilibrium shape for clusters over 28 atoms.[25] As an initial look at the structure of these clusters, we calculated the radial distribution function $g(r)$ for the largest clusters (480 atoms) across our temperature range. This was used to obtain the mean bond length from the position of first peak and the maximum bond stretch (nearest-neighbor cutoff)

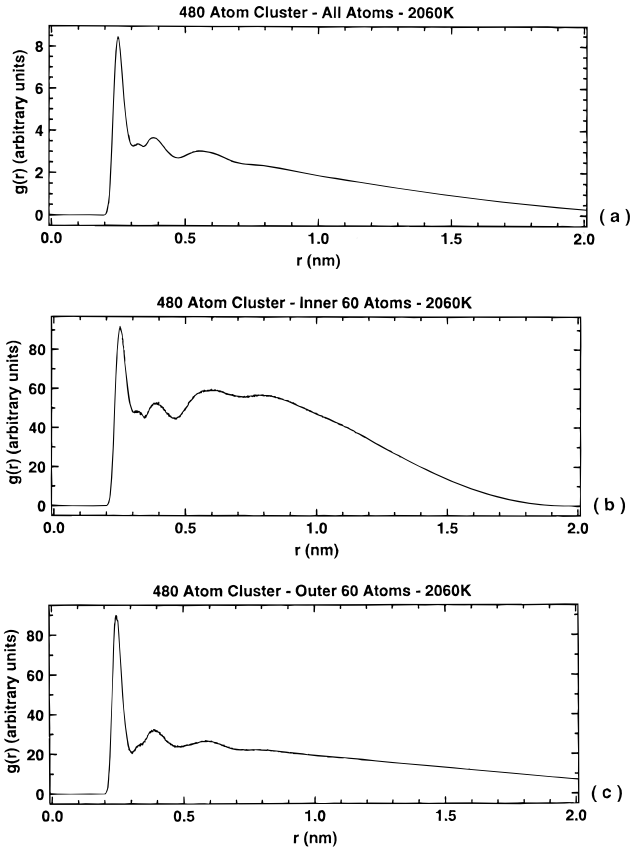

Figure 1. Pair correlation function of the 480-atom cluster at $T = 2060$ K for (a) all 480 atoms, (b) the inner 60 core atoms, and (c) the outer 60 surface atoms.

from the location of the first minimum. For the hottest clusters at 2060 K there are two minima of about equal depth between the first and second peak instead of one (Figure 1a). The locations of the two minima at 0.306 and 0.343 nm are in agreement with those obtained for bulk solid and bulk liquid silicon, respectively.[31] To test whether this finding was related to bulk and surface effects, the radial distribution function was calculated for both the 60 innermost (Figure 1b) and the 60 outermost atoms of the cluster (Figure 1c). For the inner core atoms, the first of the two minima has been replaced by a shoulder on the right-hand side of the first peak, leaving a first minimum at 0.345 nm similar to those calculated by Stillenger and Weber in molten silicon at 0.340 nm (2054 K)[31] and by Kluge et al. at 0.335 nm (1850 K).[32] For the surface atoms, the structure displays the characteristic second peak of the underlying liquid and resembles an amorphous material. Clusters at 650 K show a better resolved $g(r)$ (Figure 2a). However, there is little difference in the $g(r)$ between the core (Figure 2b) and surface atoms (Figure 2c), and both display a clear amorphous structure.

Differences between core and surface atoms are also seen in the calculation of the coordination number. The coordination number is determined from the nearest-neighbor cutoff distance obtained from the $g(r)$ and averaged over the number of neighbors each atom has within that radius. Figure 3 shows that the surface atoms are between 3- and 4-coordinated over the temperature range studied while the inner atoms are close to 5-coordinated at temperatures up to 1600 K. The 2060 K cluster shows a jump in coordination for the core atoms to 8.49, which is reasonably close to the value of 8.07 obtained by Stillinger and Weber for bulk molten silicon at 2054 K[31] and indicates that the hottest clusters are liquidlike. The mean bond length increased with temperature as expected but also showed

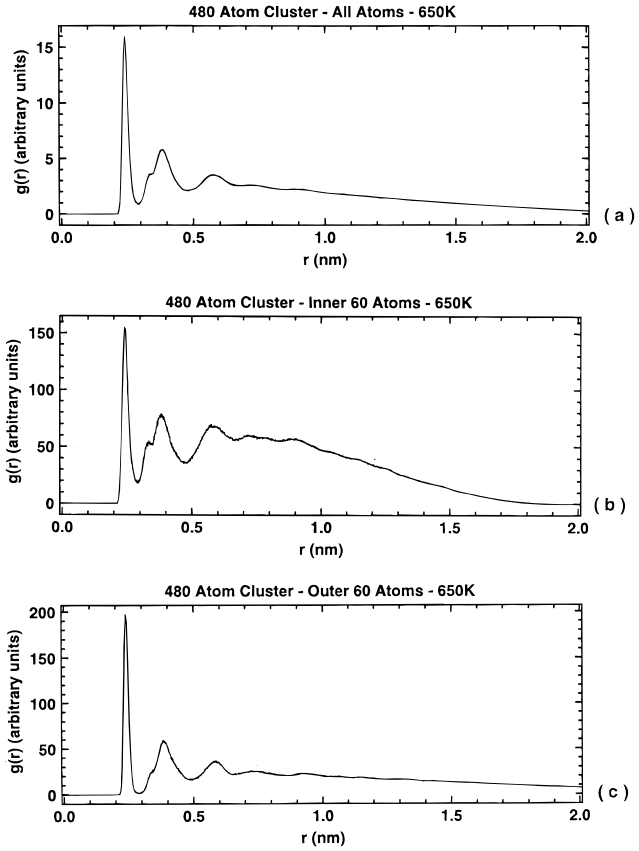

Figure 2. Pair correlation function of the 480-atom cluster at $T = 650$ K for (a) all 480 atoms, (b) the inner 60 core atoms, and (c) the outer 60 surface atoms.

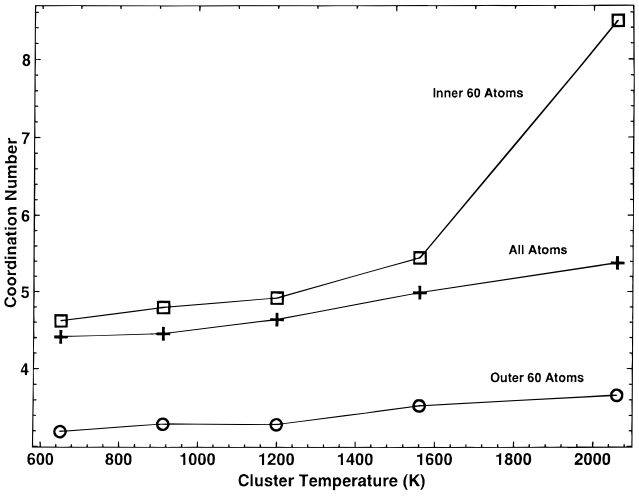

Figure 3. Average coordination number for a 480-atom cluster as a function of temperature for all 480 atoms, the inner 60 core atoms, and the outer 60 surface atoms.

differences between surface and core atoms with the core atoms having a larger bond length to accommodate higher coordination numbers. The latter result was consistent with the mean bond angle shown in Figure 4 which showed that surface atoms had bond angles closer to tetrahedral (109°). As the clusters are heated, the bond angles decrease in order to accommodate increased coordination.

Cluster Structure: Composition. Due to the large temperature range these simulations span, clusters can exist in one of the following states: liquid, glass, crystal, or amorphous. In classifying the clusters, we looked at several quantities: the radial distribution function, bond angle distribution, and mean

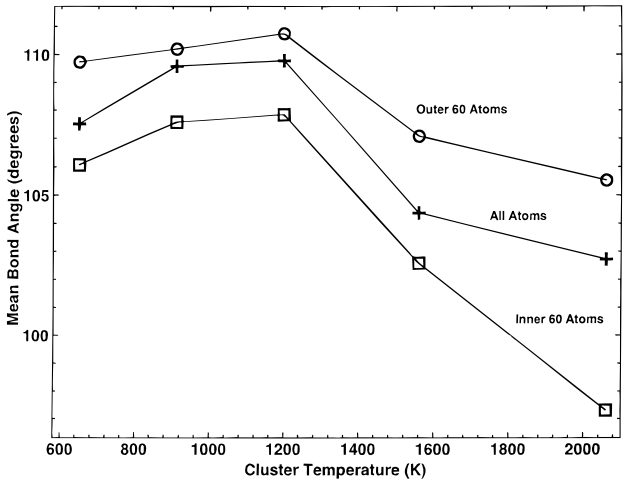

Figure 4. Mean bond angle for a 480-atom cluster as a function of temperature for all 480 atoms, the inner 60 core atoms, and the outer 60 surface atoms.

TABLE 1: Coordination Distribution As Calculated by Luedtke and Landman for Bulk Silicon[33,34]

coordination	amorphous (352 K)	glass (352 K)	crystal (352 K)	liquid (1665 K)
3	0.005	0.002	0	0.023
4	0.878	0.410	1	0.294
5	0.115	0.522	0	0.477
6	0.003	0.066	0	0.185
7	0	0.001	0	0.021
av coordn		4.66	4.00	4.89
neighbor cutoff, nm				0.2933
mean bond angle, deg	108.3 ± 14.7	106.6 ± 22.6	109.4 ± 2.7	103.9 ± 26.8

TABLE 2: Coordination Distribution Calculated in This Work for the 60-Atom Inner Core of a 480-Atom Cluster

coordination	650 K	1560 K	2060 K
3	0.006	0.002	0
4	0.438	0.127	3.8×10^{-4}
5	0.492	0.417	0.009
6	0.062	0.341	0.060
7	0.002	0.099	0.166
8	0	0.012	0.276
9	0	0	0.258
10	0	0	0.154
11	0	0	0.060
12	0	0	0.014
av coordn	4.62	5.45	8.49
neighbor cutoff, nm	0.291	0.301	0.345
mean bond angle, deg	106.8	102.59	97.31

coordination number distribution. These were all derived from atoms at the core of the cluster to avoid the effects that the surface atoms might have on these quantities and enable a comparison with results of bulk material. Luedtke and Landman[33,34] simulated bulk silicon using the SW potential and classified the states of the material by coordination number distribution and mean bond angle (Table 1). In their calculations, amorphous, glassy, and crystal materials were prepared at 352 K, while the liquid was characterized at the melting point (1664 K). The crystal state was characterized as every atom having four bonds, while amorphous material had about 10% of five bonded atoms and the "glass" is about 50% 5-coordinate. The liquid state at the melting point shows similar behavior to the glass in that the majority of atoms are 5-coordinate. Comparing the Luedtke−Landman (L−L) results as presented in Table 1 with our results for the 60 interior atoms of the 480-atom clusters in Table 2 shows good agreement between the "bulk" atoms of our 650 K cluster and the bulk L−L "glassy"

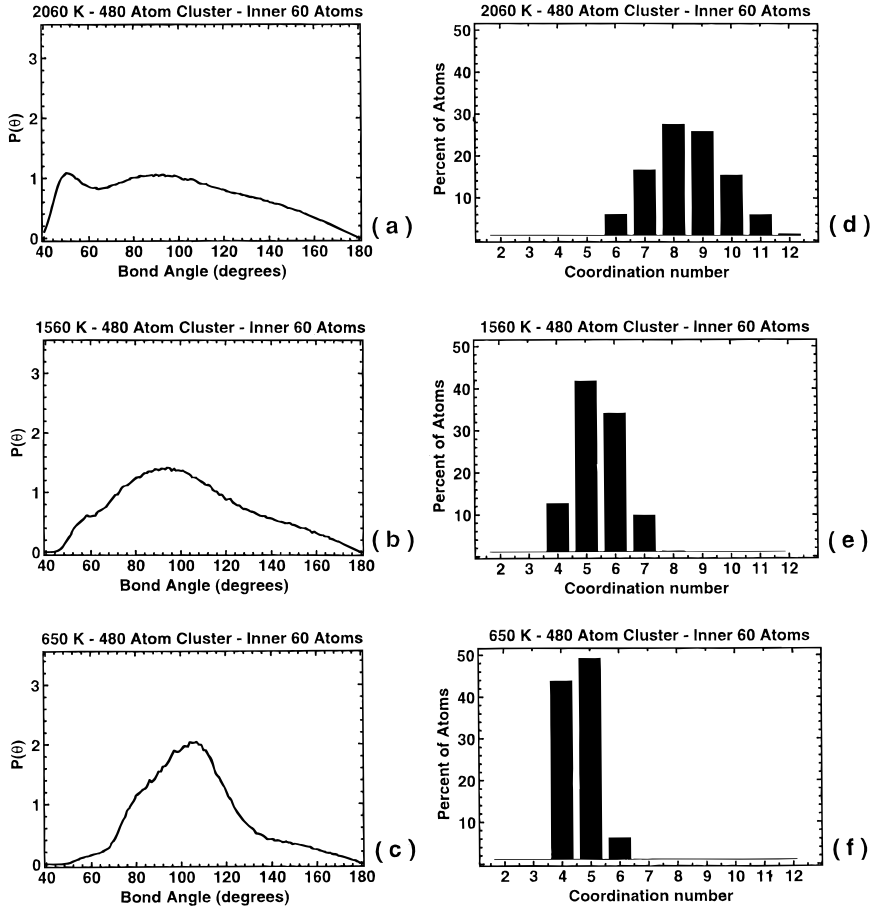

Figure 5. Bond angle distribution for the inner 60 atoms of a 480-atom cluster for (a) 2060, (b) 1560, and (c) 650 K. Coordination distribution for the inner 60 atoms of a 480-atom cluster for (d) 2060, (e) 1560, and (f) 650 K.

solid. The formation of a "glassy" or supercooled liquid cluster rather than amorphous material was expected because of the inability to quench liquid silicon to an amorphous state using the SW potential as reported by Broughton and Li.[35] While there is a reasonable match between our 1560 K cluster and the L−L material at the melting point (1665 K), the cluster at 2060 K is far into the liquid state and the coordination distribution matches that reported by Stillenger and Weber for bulk liquid.[31]

These high-temperature structural trends are more clearly revealed in Figure 5a−f which indicate the evolution of the bond angle distribution and the coordination number with increasing temperature. Bond angle distributions shown in Figure 5a−c indicate that as the temperature increases, smaller bond angles are increasingly favored, consistent with the increased coordination number as the material becomes more compact. The coordination distribution for the 2060 K cluster shows that the majority of the atoms are 8- and 9-coordinated with a mean of 8.49, in reasonable agreement with a mean coordination number of 8.07 calculated by Stillinger and Weber[31] at 2062 K. Kluge et al.[32] found an average coordination number of 7.7 with an 1850 K liquid. They also found only 0.5% of the atoms at this temperature had four bonds, in agreement with our calculations where only 0.04% of the atoms were 4-coordinated.

Since the melting point is known to vary with cluster size, for simplicity of terminology, when we refer to solid and liquid clusters, "solid" will refer to the ∼600 K glassy or supercooled liquid, while "liquid" will refer to the molten ∼2000 K material which is in fact several hundred degrees above the melting point.

For tetrahedrally bonded materials such as silicon, the atoms on the surface have a coordination number of 3 if no surface reconstruction takes place. Figure 6a shows that the outer 60

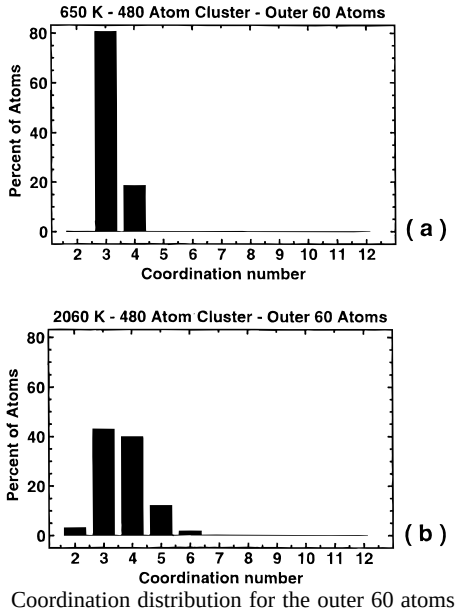

Figure 6. Coordination distribution for the outer 60 atoms of a 480-atom cluster for (a) 650 and (b) 2060 K.

surface atoms of our 650 K, 480-atom cluster has 81% 3-coordinate and 19% 4-coordinate atoms, giving us a mean coordination number of 3.2. For liquidlike clusters we should expect that the surface atoms will exhibit a coordination number larger than 3 and presumably extensive location reaccommodation of the outer atoms. Figure 6b shows that, for the outer 60 surface atoms of the 2060 K, 480-atom cluster, the number of 3-coordinated atoms has dropped to 43% and 4-coordinated atoms doubled to 40%, giving a mean coordination number of 3.7.

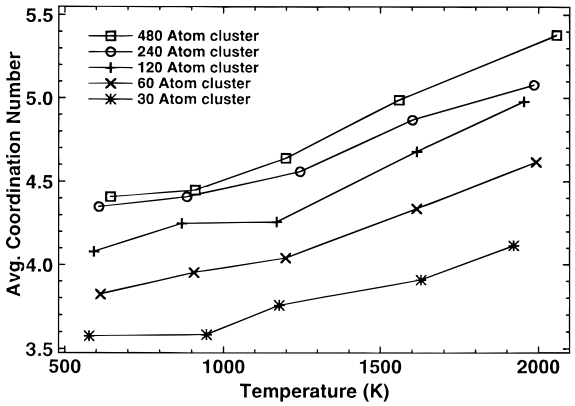

Figure 7. Average coordination number as a function of temperature and cluster size.

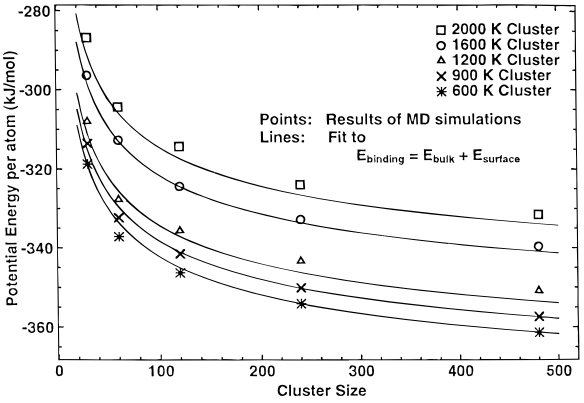

Figure 8. Dependence of cluster binding energy per atom on cluster size (N atoms) for five different temperatures. (Solid lines are fits from eq 2.)

The average coordination numbers for all cluster sizes considered in our simulations are shown in Figure 7. On average there is a gradual increase in the coordination number as temperature is increased for all clusters. The average calculated coordination number for liquid clusters is considerably lower than the experimental value of 6.4 for the bulk[36,37] due to the large number of surface atoms relative to bulk, while solid clusters have effectively reached a 4-coordinate state by 240 atoms. The most sensitive effect on average coordination number is in fact cluster size, which shows a rapid rise in coordination number as the size of the cluster increases, consistent with the rise in the percentage of bulk relative to surface atoms as the cluster gets larger.

Equilibrium Cluster Energetics. Because of the large surface-to-volume ratio, cluster properties vary with size. Indeed, this is one of the factors that presumably make nanoscale materials so interesting. The approach to bulk properties as cluster size is increased is in general specific to the property of interest. Figure 8 shows the effect of cluster size on binding energy per atom for various temperatures. Increasing the size of a spherical cluster results in a monotonically increasing cluster binding energy in agreement with the work of Kaxiras and Jackson.[25] Freund and Bauer[38] have discussed the relationship between cluster binding energy and cluster size for metal clusters and obtained a $N^{-1/4}$ relationship for the surface contribution to the binding energy per atom, based on a number of independent experimental measurements. Northby[39] has shown that for Lennard-Jones clusters, which are close-packed, there is a crossover from icosahedral configurations into fcc when about 14 atomic shells surround a central atom. For these classes of materials, surface atoms keep a coordination number between 6 and 7 and as clusters grow in size the surface

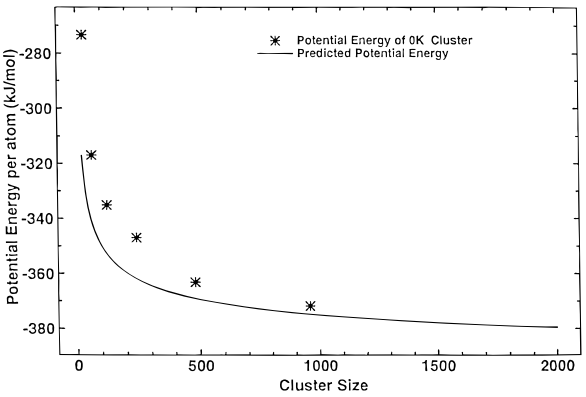

Figure 9. Binding energy per atom at 0 K versus cluster size (N). Comparison of the predicted values in this work with binding energies of spherical clusters in the perfect diamond structure (∗).

contribution to the binding energy per atom tends to vanish as $N^{-1/3}$. In contrast, for network type materials (such as silicon), atomic shells cannot be defined, but rather coordination shells need to be identified. In particular, small silicon clusters of fewer than 10 atoms are thought to be metallic in nature,[13,14] while the bulk material is covalent.[23] Several estimates have been made to determine the transition from metallic to covalent bonding and range from as few as 50 atoms[23] to as many as 4000 atoms;[13] however, none of these works describe the size dependence of the energy contribution to the binding energy.

An analysis of data in Figure 8 allows us to propose a fit to an expression showing the relative importance of bulk (volume) and surface energy (surface area) contributions to the total binding energy as follows

$$\text{binding energy} = E_b + E_s \tag{2}$$

where the bulk contribution E_b is negative and the surface contribution E_s is positive. If a cluster with N atoms is assumed to be spherical, then the binding energy per atom is given by

$$\text{binding energy}/N = \epsilon_b(T) + 4\pi r_{ws}{}^2\sigma(T)N^{-1/3} \tag{3}$$

where the bulk binding energy ϵ_b and the surface tension σ depend only on temperature. In eq 3, r_{ws} is the Wigner−Seitz radius[40] which for silicon is 1.68 Å, consistent with the lattice constant a = 5.43 Å of the diamond structure. We have assumed r_{ws} to be independent of temperature. From our results in Figure 9 we can extract a dependence of the surface tension with temperature and extrapolate the value of the bulk binding energy at zero temperature. Since this is a classical calculation, the equipartition of energy should apply and thus you get a bulk binding energy which is dependent only on temperature and not cluster size

$$\epsilon_b(T) = \epsilon_b(0) + C_v T \tag{4}$$

where $\epsilon_b(0)$ is the bulk binding energy at zero temperature and C_v is the constant-volume heat capacity. The size independence of the binding energy is shown in Figure 12 where you see that the inner atoms all have the same binding energy for each of the four cluster sizes. Below the melting temperature the potential energy contributes $C_v/R = 3$ as for any crystal. The best temperature dependence of the surface tension was obtained by utilizing an expression of the following form:

$$\sigma(T) = \sigma_0\{1 + A(1 - T/B)\exp[(T - T_m)/T_m]\} \tag{5}$$

where σ_0 is the surface tension at zero temperature, $A = 0.068$,

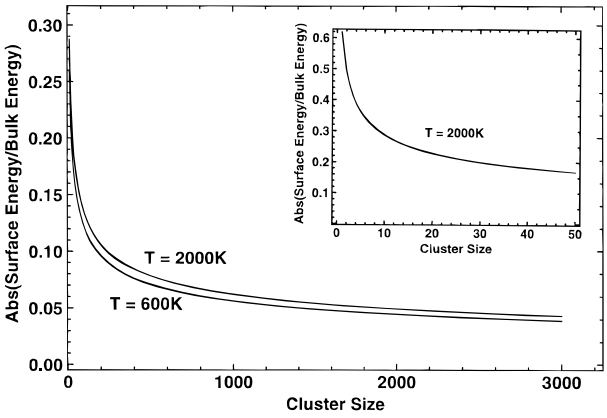

Figure 10. Comparison of surface to the bulk binding energy as a function of cluster size (*N* is the number of atoms in the cluster) for two temperatures.

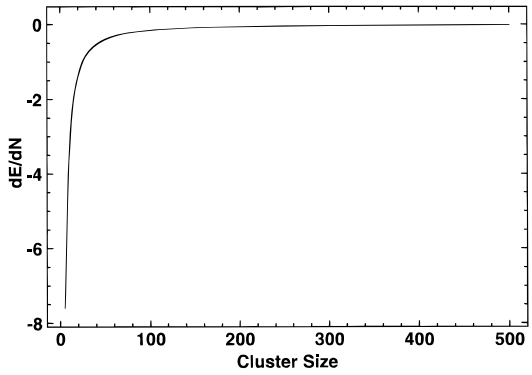

Figure 11. Derivative of potential energy function per atom as a function of cluster size.

TABLE 3: Predicted Values of Cluster Properties

property	calculated values, this work	bulk values, exptl
$\epsilon_{b(0)}$, kJ/mol	−396.7	−418
σ_0, J/m^2	0.985	0.73 at $T > 1713$ K
T_m, K	1500	1713
C_v/R	3.0 if $T < T_m$	3.0 if $T < T_m$
	4.1 if $T > T_m$	3.2 if $T > T_m$
T_c, K	6350	6400

and $B = 4000$ K and the critical temperature is obtained when $\sigma(T_c) = 0$. From the fit to our computer experiment data of Figure 9 using eqs 4 and 5, we obtained values for $\epsilon_b(0)$, σ_0, T_m, T_c, and C_v, which we list in Table 3. The value of $\epsilon_b(0)$ indicates that the material growth at these cluster sizes is not perfectly tetrahedral, but rather resembles a glassy material.

Using eqs 3 and 4 we can predict the effects of size on the binding energy at zero temperature. This calculation, is shown in Figure 9 (solid line), and compares our predicted SW potential results for the binding energies of rigid spherical clusters with a diamond structure (asterisks). It is apparent that growth following a nondiamond type is favored for clusters up to 2000-atom, whereapon a crossover occurs favoring growth corresponding to that of bulk silicon. Actual growth conditions are usually kinetically driven and may not follow the most thermodynamically favored state.

The continuous lines in Figure 8 show the result of a best fit of eq 3 using the parameters in Table 3. These results indicate that the molecular dynamics simulations can be fit quite nicely to such an expression. The bulk energy contribution to the clusters total potential energy becomes more negative as the cluster size is increased (increasing stability), while the surface term shows a shallow positive increase. In Figure 10 the absolute value of the ratio of surface to bulk energy at 600 and 2000 K obtained from eq 3 indicates the relative importance of these two contributions as a function of both temperature and cluster size. The results show that, in the temperature range explored, increasing temperature causes an increase in the *E*s/*E*b. Increasing cluster size decreases the surface-to-volume ratio and results in a decrease in the relative importance of the surface energy. Under all conditions calculated here, the cluster binding energy was negative which implies that the clusters were always stable even at high temperatures (2000 K). Extrapolation of eq 3 to cluster sizes fewer than about 30 atoms is strictly not correct since it is well-known that SW does a poor job of describing very small cluster geometries; however, from a qualitative perspective, extrapolation to small sizes (Figure 10 insert) shows that the bulk term dominates over the surface term even for a single silicon atom. The implications are that cluster growth for temperatures up to at least 2000 K will not be limited by a thermodynamic barrier.

The approach to bulk behavior is one of the most interesting aspects to the understanding of nanostructured materials, which encompasses mechanical, optical, and chemical properties. One aspect of the approach to bulk behavior is the behavior of the average binding energy per atom as a function of cluster size as we showed in Figure 9. Alternatively, we can observe the incremental change in the cluster binding energy as a function of cluster size. This is shown in Figure 11 and indicates that an asymptote is rapidly reached by a cluster of only about 200 atoms.

The potential energy of the cluster may be partitioned into a site energy associated to each atom. The instantaneous atomic binding energy as a function of an atom's position relative to the center of mass of the cluster provides a view of the relative energies of surface and interior atoms. Figure 12 shows an instantaneous snapshot of site energies for four cluster sizes at 600 K. These solid clusters show common features of a tightly bound inner core enveloped by less strongly bound surface atoms whose binding energy is approximately 80% of that for the inner atoms. Most interesting is the fact that outer atoms do not seem to show any cluster size dependence to their binding energy. Indeed, one might expect that cluster properties which are so dependent on size would be sensitive to this parameter. The indications are that size dependence may be more a function of the relative amount of bulk and surface atoms rather than the exact nature of the surface, at least on the level of these calculations where no electronic effects are accounted for. Liquid clusters at 2000 K display a similar behavior to that of the solid clusters shown in Figure 12, with the exception that the distinction between inner and surface atoms is blurred. A similar analysis for the instantaneous kinetic energy shows no distinctive features as one progresses from the center to the outer edge of the cluster, consistent with a good equilibration.

Figure 13 shows the instantaneous site energy broken down by the site coordination number as a function of distance from the center of mass for the 600 K, 480-atom cluster. Consistent with the results of Figure 3, outer atoms have the lowest coordination number and smallest bond length and are also the atoms with the lowest binding energy. As one moves to the interior of the cluster, the coordination number increases along with the binding energy. Such an analysis is not so easily constructed for the 2000 K clusters because of their high atomic mobility.

Vibrational Energy. Vibrational energy transfer processes are very important to the mechanism of cluster stabilization during growth as well as its radiative properties. The vibrational density of states was calculated by taking the FFT of the velocity

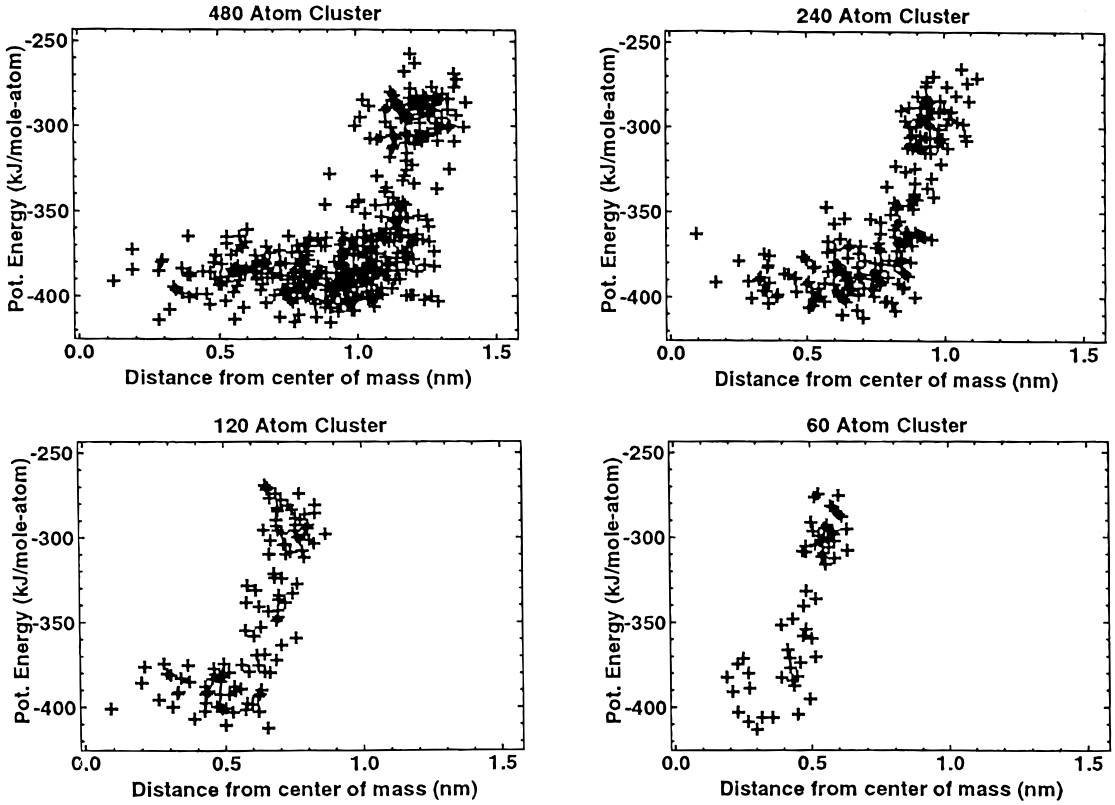

Figure 12. Instantaneous atomic binding energy as a function of position relative to the center of mass for four different cluster sizes at 600 K.

autocorrelation function $C(t)$:

$$\frac{1}{N}\langle\sum_{i=1}^{N}\mathbf{v}_i(t_0)\cdot\mathbf{v}_i(t_0+t)\rangle \tag{6}$$

Figure 14 shows the density of vibrational states of the 480-atom cluster as a function of cluster temperature. A comparison with the calculated phonon density of states for bulk silicon[41] is also included in the insert of Figure 14. It is clear that the density of vibrational states is not significantly altered as a result of the large number of surface atoms. The spectra show the two dominant modes found in bulk silicon (acoustic, 150 cm^{-1}; optical, 400 cm^{-1}). As the cluster temperature is increased, the phonon density displays broadening and a softening of the modes to lower frequencies. The density of vibrational states does not show a major discernible size dependence.

Silicon Self-Diffusion Coefficients. Self-diffusion coefficients have been calculated from the mean-square displacement (MSD) from eq 7:

$$\mathrm{MSD} = \frac{1}{N}\sum_{i=1}^{N}[\mathbf{r}_i(t) - \mathbf{r}_i(0)]^2 \tag{7}$$

$$\mathrm{MSD} = 6D/t \tag{8}$$

Figure 15 shows calculations of the MSD in a 480 atom-cluster (at 600, 1200, and 2000 K) as a function of time. The curvature in the MSD toward an asymptote results from the finite nature of the cluster. The diffusion coefficient can be evaluated from the initial slope of the MSD (eq 8).

Figure 16 shows the calculated diffusion coefficients as a function of temperature and cluster size. The non-Arrhenius behavior is suggestive of a phase change over the temperature range sampled.

Because clusters of this size are essentially composed of surface rather than volume type atoms, comparison with experiment is most appropriate with surface self-diffusion data. Unfortunately, such data are scarce and of questionable accuracy. The most direct measurement has been made by Makowiecki and Holt,[42] who reported a silicon surface diffusion constant of 4×10^{-8} cm^2/s at 1273 K. Our data for the largest cluster (480 atoms) gave a diffusion constant of about 1×10^{-5} cm^2/s at 1270 K, which is significantly larger than the experimental results, indicating liquidlike behavior at lower temperatures than bulk surfaces. Mo et al.[43] did a high-quality STM study at lower temperatures, which we have extrapolated to the range of temperatures we have studied. The comparison is quite good as is that for the Robertson[44] work which crosses our data, all be it with a different activation energy. Clearly there exists substantial discrepancy within the bulk experimental data, with no obvious way to access the accuracy of the results. Certainly, it is well-known that the Stillinger−Weber potential underpredicts the binding energy in bulk silicon which would tend to increase the computed surface diffusion coefficient. On the other hand, the tight binding molecular dynamics study of Wang et al.[45] for liquid silicon at 2000 K agrees quite well with our calculated diffusion coefficient of the largest cluster used (480 atoms) at the same temperature. The most obvious source of error in the experiment, namely surface oxidation would tend to decrease the diffusion coefficient, consistent with the available data which either lie with our data or below it.

Conclusions

Classical molecular dynamics simulations using the three-body Stillinger−Weber interatomic potential have been used to simulate the equilibrium characteristics of clusters over a wide range of cluster sizes ($30 < n < 480$ atoms) and temperatures ($600 < T < 2000$ K). The structure of the innermost 60 atoms of 480 atom clusters over the entire temperature range were found to resemble that of bulk "glassy" silicon. Three distinct phases for these clusters were observed. At low temperatures (650 K) the cluster was found to correspond to a "glass" or

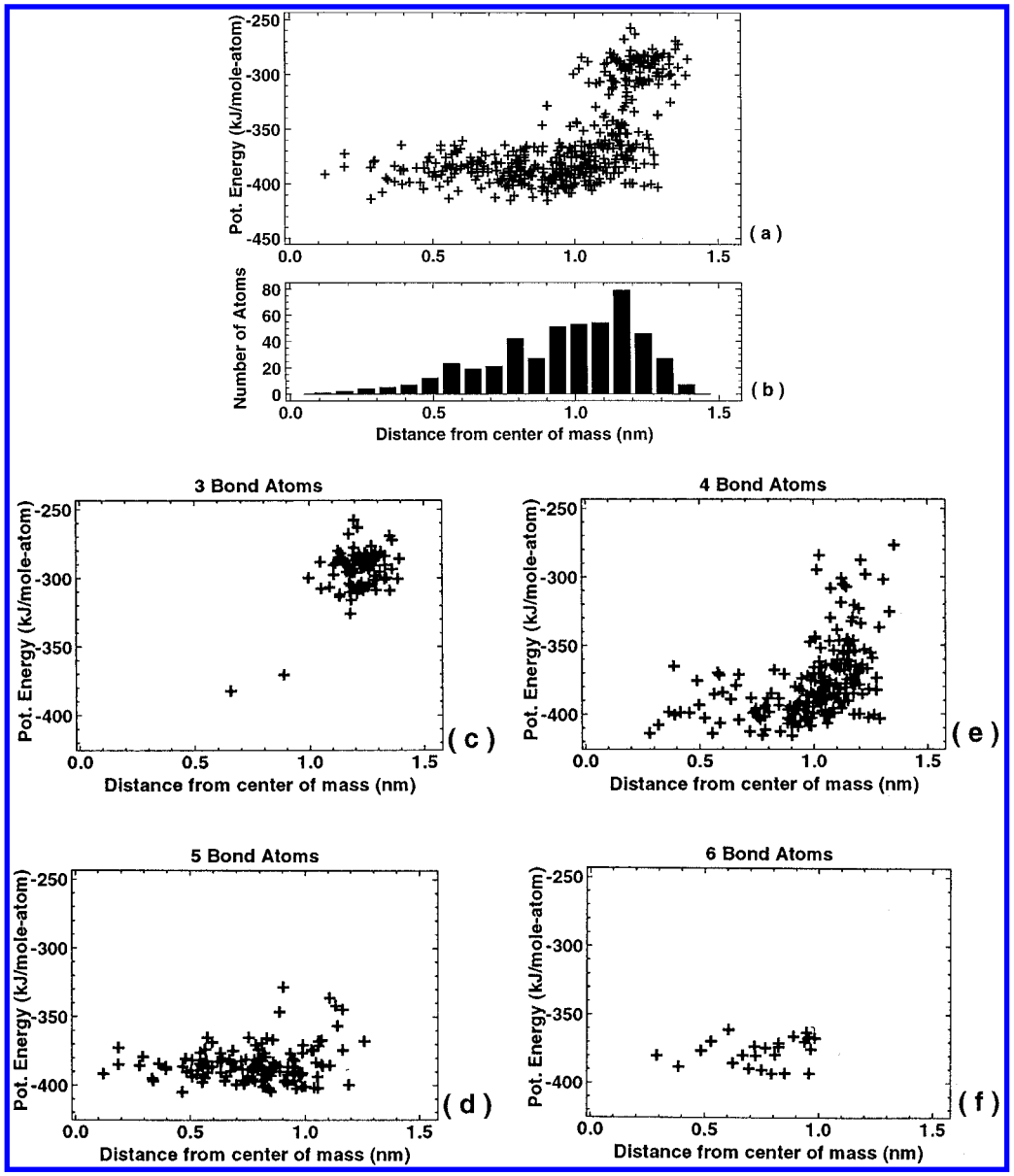

Figure 13. (a) Site energy and (b) mass distribution versus distance from center of mass for $N = 480$ cluster at $T = 600$ K. (c−f) Site energy as a function of distance from center of mass for the atoms with coordination 3−6, respectively.

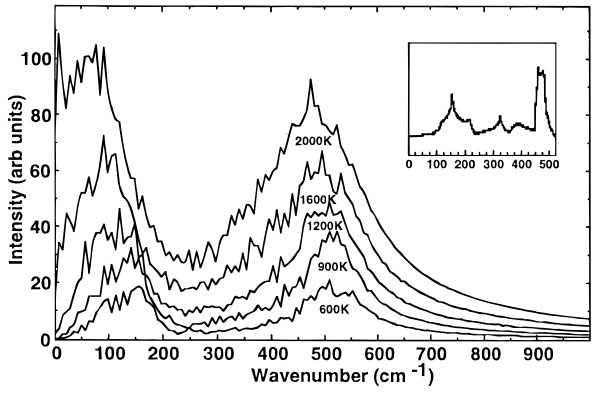

Figure 14. Phonon density of states for a 480-atom cluster as a function of cluster temperature.

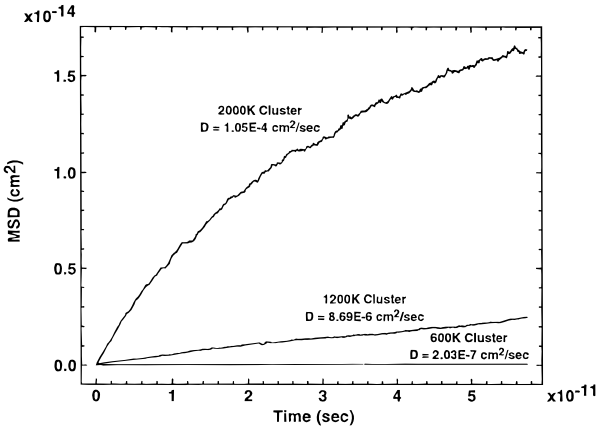

Figure 15. Mean-square displacement of atoms as a function of time.

supercooled liquid as observed by Ludetke and Landman,[33,34] while at the melting point (1560 K) the cluster showed a coordination distribution corresponding again to the Ludetke and Landman study for bulk silicon at the melting point (1665 K). At still higher temperatures (>2000 K), cluster structures corresponded quite closely to those calculated by Stillinger and Weber for bulk liquid silicon at 2054 K.[31]

Cluster binding energy calculated as a function of size and temperature have been fitted to an expression that accounts for bulk and surface contributions. The cluster results as compared

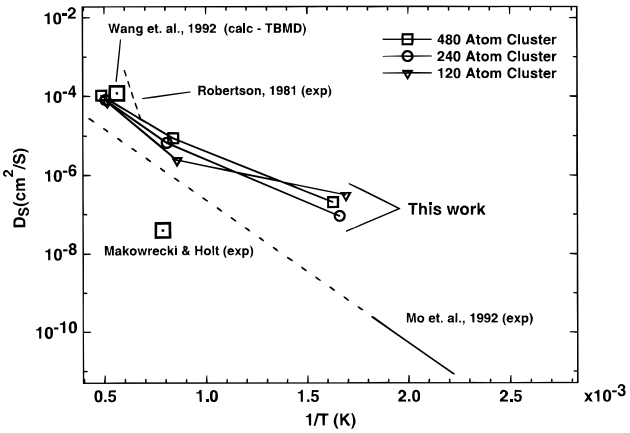

Figure 16. Arrhenius plot of self-diffusion coefficients versus inverse of temperature.

with bulk properties are consistent. Growth seems to be through glass-like rather than crystalline structures. Phonon density spectra show no outstanding features when compared to the bulk implying that thermal transport properties within the clusters should be similar. Calculated self-diffusion coefficients show that cluster results are similar to experimental data of bulk surfaces at intermediate temperatures and the diffusion coefficients for large clusters at high temperatures agree with values of a bulk liquid.

References and Notes

(1) Xiong, Y.; Pratsinis, S. E. *J. Aeros. Sci*. **1992**, *22* (Suppl. 1), 199.
(2) Gelbard, F.; Tambour, Y.; Seinfeld, J. H. *J. Colloid Interface Sci*. **1980**, *76*, 541.
(3) Zachariah, M. R.; Semerjian, H. G. *AIChE. J*. **1989**, *35*, 2003.
(4) Zachariah, M. R.; Dimitriou, P. *Aeros. Sci. Technol*. **1990**, *13*, 413.
(5) Zachariah, M. R.; Aquino, M. I.; Shull, R. D.; Steel, E. B. *Nanostructured Mater*. **1995**, *5*, 383. McMillin; B. K.; Biswas, P.; Zachariah, M. R. *J. Mater. Res.* **1996**, *11*, 1552.
(6) Kahn, F. S.; Broughton, J. Q. *Phys. Rev. B* **1989**, *39*, 3688.
(7) Sankey, O. F.; Niklewski, D. J.; Drabold, D. A.; Dow, J. D. *Phys. Rev. B* **1990**, *41*, 12751.
(8) Ballone, P.; Andreoni, W.; Car, R.; Parrinello, M. *Phys. Rev. Lett*. **1988**, *60*, 271.
(9) Maluendes, S. A.; Dupuis, M. *Int. J. Quantum Chem*. **1992**, *42*, 1327.
(10) Fueston, B. P.; Kalia, R. K.; Vashista, P. *Phys. Rev. B* **1988**, *37*, 6297.
(11) Mistriotis, A. D.; Froudakis, G. E.; Vendras, P.; Flytzanis, N. *Phys. Rev. B* **1993**, *47*, 10648.
(12) Balmane, H.; Halicioglu, T.; Tiller, T. A. *Phys. Rev. B* **1992**, *46*, 2250.
(13) Tomanek, D.; Schluter, M. *Phys. Rev. Lett*. **1986**, *56*, 1055.
(14) Raghavachari, K. *J. Chem. Phys*. **1985**, *83*, 3520.
(15) Raghavachari, K. *J. Chem. Phys*. **1986**, *84*, 5672.
(16) Tchofo Dinda, P.; Vlastou-Tsinganos, N.; Flytzanis, N.; Mistriotis, A. D. *Phys. Lett. A* **1994**, *191*, 339.
(17) Andreoni, W.; Pastore, G. *Phys. Rev. B* **1990**, *41*, 10243.
(18) Feuston, B. P.; Kalia, R. K.; Vashishta, P. *Phys. Rev. B* **1987**, *35*, 6222.
(19) Gong, X. G. *Phys. Rev. B* **1993**, *47*, 2329.
(20) Binggeli, N.; Chelikowsky, J. R. *Phys. Rev. B* **1994**, *50*, 11764.
(21) Blaisten-Barojas, E.; Levesque, D. *Phys. Rev. B* **1986**, *34*, 3910.
(22) Blaisten-Barojas, E.; Zachariah, M. R. *Phys. Rev. B* **1992**, *45*, 4403.
(23) Chelikowsky, J. R. *Phys. Rev. Lett*. **1988**, *60*, 2669.
(24) Rothlisberger, U.; Andreoni, W.; Parrinello, M. *Phys. Rev. Lett*. **1994**, *72*, 665.
(25) Kaxiras, E.; Jackson, K. *Phys. Rev. Lett*. **1993**, *71*, 727.
(26) Kaxiras, E.; Jackson, K. *Z. Phys. D* **1993**, *26*, 346.
(27) Biswas, R.; Hamann, D. R. *Phys. Rev. B* **1986**, *34*, 895.
(28) Kobayashi, K.; Nagase, S. *Bull. Chem. Soc. Jpn*. **1993**, *66*, 3334.
(29) Wales, D. J.; Waterworth, M. C. *J. Chem. Soc., Faraday Trans*. **1992**, *88*, 3409.
(30) Verlet, L. *Phys. Rev.* **1967**, *159*, 98.
(31) Stillinger, F. H.; Weber, T. S. *Phys. Rev. B* **1985**, *31*, 5262.
(32) Kluge, M. D.; Ray, J. R. *Phys. Rev. B* **1987**, *36*, 4234.
(33) Luedtke, W. D.; Landman, U. *Phys. Rev. B* **1988**, *37*, 4656.
(34) Luedtke, W. D.; Landman, U. *Phys. Rev. B* **1989**, *40*, 1164.
(35) Broughton, J. Q.; Li, X. P. *Phys. Rev. B* **1987**, *35*, 9120.
(36) Waseda, Y.; Suzuki, K. *Z. Phys. B* **1975**, *20*, 339.
(37) Gabathuler, J. P.; Steeb, S. *Z. Naturforsch*. **1979**, *34a*, 1314.
(38) Freund, H. J.; Bauer, S. H. *J. Phys. Chem*. **1977**, 81.
(39) Northby, J. A. *J. Chem. Phys*. **1987**, *87*, 6166.
(40) Kittel, C. *Introduction to Solid State Physics*; John Wiley: New York, 1965.
(41) Weber, W. *Phys. Rev. B* **1977**, *15*, 4789.
(42) Makowiecki, D. M.; Holt, J. B. *Mater. Sci. Res*. **1979**, *13*, 279.
(43) Mo, Y. W.; Kleiner, J.; Webb, M. B.; Lagally, M. G. *Surf. Sci*. **1992**, *268*, 275.
(44) Robertson, W. M. *J. Am. Ceram. Soc*. **1981**, *64*, 9.
(45) Wang, C. Z. *Phys. Rev. B* **1992**, *45*, 12227.

JP953773W